European Journal of Pharmaceutics and Biopharmaceutics 142 (2019) 396–404

Contents lists available at ScienceDirect

European Journal of Pharmaceutics and Biopharmaceutics

journal homepage: www.elsevier.com/locate/ejpb

Research paper

Scale-Up of pharmaceutical Hot-Melt-Extrusion: Process optimization and transfer

Jens Wesholowski[a], Kevin Hoppe[a], Kathrin Nickel[b], Christian Muehlenfeld[c], Markus Thommes[a,*]

[a] Laboratory of Solids Process Engineering, TU Dortmund University, Dortmund, Germany
[b] Leistritz AG, Nuremberg, Germany
[c] Ashland Industries Deutschland GmbH, Duesseldorf, Germany

ARTICLE INFO

Keywords:
Process analytical technology
Process optimization
Residence time
Scale-Up
Twin-Screw-Extrusion

ABSTRACT

Hot-Melt-Extrusion on Twin-Screw-Extruders has been established as a standard processing technique for pharmaceutical products. A major challenge is the transfer from a lab to a production level, since the combination of several unit operations within one apparatus leads to complex conditions for such a continuous manufacturing process. Here the residence time distribution is a crucial measure, which reflects the different mechanisms, e.g. dissolution, mixing or degradation, during processing. In the first part of a Scale-Up study, a methodology for the optimization of an extrusion process with respect to the load and throughput is presented. The developed concept was applied for different extruder scales in order to compare the identified processing windows. A deviation of the dominant material heating mechanisms was observed for the different scales, while the constraints for the transfer of a process to a different scale by the developed optimization concept is demonstrated. Finally, a sufficient operating point on a reference extruder is identified and in the second part of this study, different concepts from literature are applied for the transfer of this Hot-Melt-Extrusion process to two larger scales. The focus of the investigations was on the impact of the different approaches on the residence time distribution and the comparison. The determined results revealed a change of the most sufficient approach for the two different extruder sizes. The impact on the location in the time domain and form of the distribution are discussed and additionally evaluated by the fit to a RTD-model. In conclusion, the ratio of the applied energy for transport to mixing is identified as valuable addition in this context.

1. Introduction

Within the last decade Twin-Screw-Extrusion (TSE) has been a focus of research interest within the field of pharmaceutical technology [1,2]. A key aspect in this context is a shift of batch production to continuous manufacturing [3,4], which is driven by the overall aim of process optimization and an enhanced cost efficiency [5]. One approach to this is the specific design of production processes based on the correlation of desired quality attributes and process parameters. The corresponding concept Quality-by-Design is based on the work of Juran from 1992 [6].

In this context, TSE offers a vast potential. Due to the modular set-up [7] and the implementation of different screw element types [8–10] several unit operations can be combined within one apparatus. This reduces the machine footprint and invest costs. At the same time, this continuous technology is robust, which reduces set-up times and enhances the overall process stability. Therefore, Hot-Melt-Extrusion (HME) with co-rotating Twin-Screw-Extruders has been a standard process for the production of solid dispersions [11]. This specific dosage form is an approach for one major challenge of the pharmaceutical industry nowadays: the bioavailability enhancement of poorly water soluble drugs [12,13].

Solid dispersions consist of a drug dispersed within a matrix, typically a polymer [14]. During HME the dissolution of the active pharmaceutical ingredient (API) within the carrier melt is crucial. An indicator for this mechanism is the residence time distribution (RTD) [15], since the on-set is a surrogate for the minimum contact time of drug and polymer melt. Additionally, the width of the distribution indicates the backmixing of material [16]. This is related to the distributive mixing performance, which is essential for product homogeneity. Finally, the off-set of the RTD symbolizes the maximum duration of thermal and mechanical stress applied to the processed material [17]. Overall, this is linked to degradation processes [18,19]. In consequence, the RTD reflects critical mechanism for extrusion.

Another major challenge for pharmaceutical technology and TSE is

* Corresponding author at: Laboratory of Solids Process Engineering, Emil-Figge-Straße 68, 44227 Dortmund, Germany.
E-mail address: markus.thommes@tu-dortmund.de (M. Thommes).

https://doi.org/10.1016/j.ejpb.2019.07.009
Received 15 January 2019; Received in revised form 1 July 2019; Accepted 6 July 2019
Available online 08 July 2019
0939-6411/

Nomenclature

A	absorbance of light as function of wavelength [–]
AUC	function integral of the residence time density function of the Twin-Dispersion-model [s]
Bo	Bodenstein-number [–]
c	concentration-function *
c_0	initial signal related to initial tracer concentration *
D_a	external screw diameter [m]
D_i	internal screw diameter [m]
E	residence time density function [s^{-1}]
EBR	energy balance rate [s^{-1}]
Fr	Froude-number [–]
g	gravitational acceleration [$m\,s^{-2}$]
L	dimensionless extruder length [m]
$\dot{m}$	total mass flow of powder inlet [$kg\,s^{-1}$]
M	motor torque [N m]
n	screw speed [kg]
SFL	specific feed load [–]
SME_{blank}	specific mechanical energy input for the operation of empty extruder [$kW\,h\,kg^{-1}$]
SME_{total}	total specific mechanical energy [$kW\,h\,kg^{-1}$]
$SME_{\Delta p}$	applied specific mechanical energy for pressure build up [$kW\,h\,kg^{-1}$]
$SME_{\Delta p+\gamma}$	applied specific mechanical energy for pressure build up and material shearing [$kW\,h\,kg^{-1}$]
SME_{γ}	applied specific mechanical energy for material shearing [$kW\,h\,kg^{-1}$]
$\bar{t}$	mean residence time [s]
t	time [s]
t_i	time to a quantile value of i% [s]
T	temperature [C]
T_{melt}	melt temperature at the extruder outlet [°C]
$T_{barrel,max}$	maximum set barrel temperature [°C]
$T_{max,set}$	set value for maximum melt temperature [°C]
Tr	transmission of light [–]
Δp	pressure build up [$10^5\,N\,m^{-2}$]
λ	wavelength [nm]
ρ	density [$kg\,m^{-3}$]

the Scale-Up [20,21] of such a production method from a lab to an industrial level. From an economic point of view, the process should be optimized regarding throughput during early stage development level in a first step in order to ensure a maximum degree of utilization for the machine. During Scale-Up the maximizing of the output should prevent unnecessary investment cost and during later production. In this context, the fill level [22] is crucial, since it is a measure for the utilization of an apparatus.

At the same time, the throughput and fill level have a direct impact on the RTD [23], which is influenced for a constant formulation by machine as well as process parameters, e.g. the screw configuration, the free volume inside the extruder, the screw speed, mass flow or temperature profile. This complexity contributes to the general challenge of a process transfer from a development stage to an industrial production level. Several Scale-Up concepts for TSE are presented within literature and can be classified in approaches related to geometric or energetic aspects. However, these are not focusing on the RTD and the variation of this parameter by the scale transfer.

The aim of this study is on the one hand to present a systematic methodology for enhancing the workload of a TSE process and finally identify a sufficient process parameter set with respect to various limitations. These are either linked to material properties, e.g. the degradation temperature, or the performance of the extruder itself, e.g. the drive power. The systematic approach is used for three machine sizes of extruders in order to highlight the universality of it, while at the same time general constraints for the application are identified. For reasons of comparability, the screw configuration was kept geometrically constant as well as the temperature profile for all experiments. Finally, the impact of maximizing the throughput on the residence time is demonstrated and compared for different extruder sizes. Therefore, the RTD is determined inline via UV–VIS spectroscopy.

The second focus of this study is to characterize the effect for different Scale-Up concepts from literature on the RTD and the individual potential for the preservation of this critical process parameter. The approaches from literature are applied for a reference point on the smallest extruder to larger machine sizes at two levels. The screw configuration was kept geometrically constant in order to emphasize the same unit operations and maintain the general process mechanisms. Correlations between direct process parameters (mass flow, screw speed) and the impact on the RTD as an indirect process parameter during Scale-Up are identified and additionally characterized by the fit to a model and the corresponding model parameters.

2. Materials and methods

2.1. Hot-Melt-Extrusion on co-rotating Twin-Screw-Extruders

The experiments were carried out on three different intermeshing, co-rotating Twin-Screw-Extruders (Leistritz, Nuremberg, Germany) from the ZSE-series with a nominal external screw diameter D_a of 17.8 mm (ZSE 18), 27 mm (ZSE 27) and 39.7 mm (ZSE 40). For all applied extruders the ratio of D_a to the inner screw diameter D_i was in the range of 1.5 and the relative length L of the processing section was 36 D_a (see Table 1). Screw configuration and temperature profile are based on a common set-up from literature [24] and were scaled geometrically similar with respect to the available screw and barrel element sizes (see Fig. 1). The material was fed gravimetrically in each case. The processed formulation consisted of the polymer copovidone (Plasdone S-630, PVP-VA, Ashland, USA) and theophylline-anhydrate (Siegfried PharmaChemikalien, Minden, Germany) as active pharmaceutical ingredient (API) with a constant drug load of 5 wt%. The blend was mixed batchwise at a lot size of 10 kg with a bin blender (SAM50S, Mixaco, Neuenraade, Germany) for 10 min at a screw speed of 200 rpm. However, for calculations the crystal density of the pure polymer at 1.27 $g\,cm^{-3}$ was considered due to the low drug concentration. The melt temperature at the outlet was determined with an IR Camera (Testo 875, Testo AG, Lenzkirchen, Germany).

2.2. Inline determination of residence time

For the determination of the RTD the marker substance quinine-dihydrochlorid (Caesar & Loretz, Hilden, Germany) was utilized at a range of 16–23 mg per mass flow of 1 $kg\,h^{-1}$ of the processed formulation. The marker was added as Dirac-impulse through the hopper and the response signal was measured in the die with an inline UV–Vis–spectrophotometer (Inspectro X, ColVisTec AG, Germany). This was executed in transmission with two probes (TPMP, ColVisTec AG, Germany) at an offset of 180°, due to the transparent appearance of the

Table 1
Specifications of the applied extruders.

Extruder	Da [mm]	Da/Di [–]	L [–]	M [Nm]
ZSE 18	17.8	1.51	36 D_a	71
ZSE 27	27.0	1.47	36 D_a	256
ZSE 40	39.7	1.55	36 D_a	830

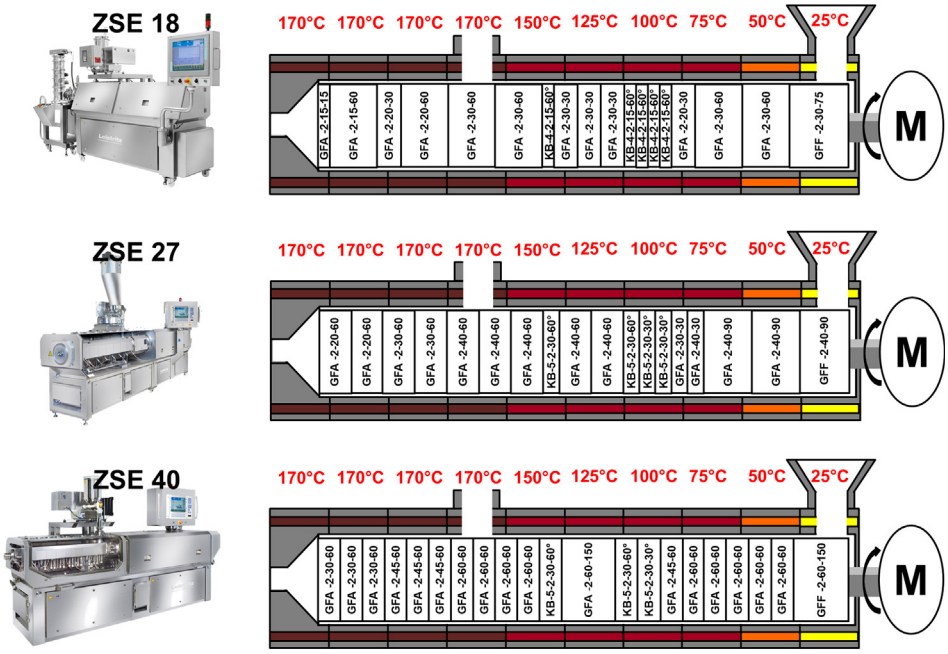

Fig. 1. Applied screw configuration and barrel temperature profile for the different extruder scales in comparison.

melt. The obtained data sets consist of the light transmission Tr as a function of the time t and wavelength λ. The effect on the spectra corresponding to the presence of quinine was located between 250 and 650 nm. The transmission expresses the ratio of light intensity I to the emitted basic light intensity I_0. This value was converted with respect to the Lambert-beer-Law into an integrated, cumulative absorbance A (Eq. (1)).

$$A_{250-650nm}(t) = \int_{250\ nm}^{650\ nm} \left(\log_{10}\frac{1}{Tr(\lambda, t)}\right)d\lambda \tag{1}$$

The obtained value was nominated by the function integral over the time. By this the residence time density function E was obtained. This is a suitable measure to compare the RTD for different set-ups, since the function integral is 1 and the corresponding function values represent an exit probability.

$$E(t) = \frac{A_{250-650\ nm}(t)}{\int A_{250-650\ nm}(t)dt} \tag{2}$$

2.3. Applied scale-up concepts

The applied Scale-Up concepts in general focus on keeping a specific process parameter constant. These are either related to geometrical aspects or the energy input and are used for the transfer from a reference (ref) to a different apparatus size (i).

Most commonly applied is the **volumetric approach (SFL)**, which concentrates on the load of the extruder represented by the specific feed load SFL [25]. This parameter considers the total mass flow in relation to the generated volume by the screw rotation. This is dependent on the screw speed n and the outer screw diameter D_a. For a dimensionless contemplation the mass flow is converted into a volume flow by the material density ρ.

$$SFL = \frac{\dot{m}}{\rho\ n\ {D_a}^3} \tag{3}$$

For a Scale-Up based on the SFL [26] a simplified correlation is derived (Eq. (4)), which assumes the screw speed and the density to be constant.

$$\dot{m}_i = \dot{m}_{ref}\left(\frac{D_{a,i}}{D_{a,ref}}\right)^3 \tag{4}$$

An **advanced volumetric approach (aSFL)** takes also the intake mechanism into account. The corresponding mechanisms are reflected by the Froude number Fr, which is defined as the ratio of inertial forces to gravitational forces [27]. For the material feeding during extrusion this is related to the screw speed n, the acceleration due to gravity g and the characteristic length D_a.

$$Fr = \frac{4\ \pi\ n^2 D_a}{g} \tag{5}$$

For a constant Fr-number the screw speed at a varied machine size is dependent on the ratio of the outer screw diameters (Eq. (6)). This also effects the adaption of the mass flow (Eq. (7)) in addition to Eq. (4).

$$n_i = n_{ref}\left(\frac{D_{a,ref}}{D_{a,i}}\right)^{0.5} \tag{6}$$

$$\dot{m}_i = \dot{m}_{ref}\left(\frac{D_{a,i}}{D_{a,ref}}\right)^{2.5} \tag{7}$$

The **heat transfer approach (HT)** [22] focuses on the applied thermal energy as a crucial objective, especially for thermal sensitive compounds [28]. A key aspect in this context is the barrel heating and the transfer over the inner barrel surface. This area results from circumference of the intermeshing screws and the length of the processing zone has to be considered as well. Both of these parameters are typically a multiple of D_a. Thus, the transferred heat energy at the surface is expressed by the heat transfer coefficient α, the Surface S and the temperature gradient between barrel and material. For a constant heating profile, formulation and barrel material for the different extruder sizes, the Scale-Up is then solely dependent on D_a (Eq. (8)).

$$\dot{m}_i = \dot{m}_{ref}\left(\frac{D_{a,i}}{D_{a,ref}}\right)^2 \tag{8}$$

In contrast to geometric approaches, the **energy input approach (SME)** is related to the expended total specific mechanical energy SME_{total} [25] for processing, which can be calculated with respect to the torque M, the screw speed n and the mass flow.

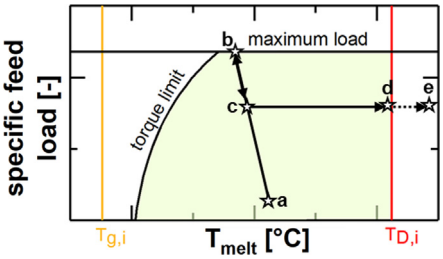

Fig. 2. Schematic course of the SIOS concept within the processing window according to the SFL and the melt temperature. Different limitations related to the material or the machine performance are considered.

$$SME_{total} = \frac{n \; M}{\dot{m}} \tag{9}$$

However, SME_{total} unites the applied energy for the operation of the empty extruder SME_{blank}, the pressure build up $SME_{\Delta p}$ and for shearing the material by the turning screws $SME_{\dot{\gamma}}$. Therefore the difference of SME_{total} to SME_{blank} symbolizes the net applied energy to the processed material $SME_{\Delta p+\dot{\gamma}}$.

$$SME_{total} - SME_{blank} = SME_{\Delta p} + SME_{\dot{\gamma}} = SME_{\Delta p+\dot{\gamma}} \tag{10}$$

The ratio of $SME_{\Delta p}$ to $SME_{\dot{\gamma}}$ represents the proportion of net applied energy for material transport to material mixing. An decrease of the energy balance rate (EBR) symbolizes an enhanced material distribution in comparison (Eq. (11)).

$$EBR = \frac{SME_{\Delta p}}{SME_{\dot{\gamma}}} \tag{11}$$

2.4. Applied RTD model

The RTD of extrusion is dominated by two mixing mechanisms during the extrusion process, which are reflected by the characteristic parameters of the Twin-Dispersion-model (TDM). This approach considers the superimposition of two functions [31] based on the Axial-Dispersion-model (ADM). The Bodenstein-number Bo as characteristic model parameter symbolizes the ratio of material flow to axial dispersion, while $\bar{t}$ is the general location parameter [33,34]. A value of Bo over 100 represents a transport mechanism close to plug flow, a value towards 0 indicates ideal mixing close to an ideal stirred tank reactor. Therefore, typically two approaches for the Axial-Dispersion model have to be distinguished for Bo ≤ 100 (Eq. (16)) and Bo > 100 (Eq. (17)).

$$E(t) = \frac{1}{2\cdot\bar{t}}\left(\frac{Bo}{\pi\frac{t}{\bar{t}}}\right)^{0.5} e^{-\frac{Bo\left(1-\frac{t}{\bar{t}}\right)^2}{4\frac{t}{\bar{t}}}} \tag{16}$$

$$E(t) = \frac{1}{2\cdot\bar{t}}\left(\frac{Bo}{\pi}\right)^{0.5} e^{-\frac{Bo\left(1-\frac{t}{\bar{t}}\right)^2}{4}} \tag{17}$$

The first function of the TD-model with Bo_1 and $\bar{t}_1$ represents material flow through the screw channel [32], which is related to plug flow and therefore the values are typically in the range of 100 and above. The second function of the TD-model with Bo_2 and $\bar{t}_2$ represents material flow within the screw-barrel clearance or screw-screw clearance. Mathematically, both functions are convoluted and nominated by the function integral AUC in order to derive the residence time density function E. Additionally, a scaling parameter in form of the concentration c_0 is considered, which represents the signal related to the initial tracer concentration. Therefore the tracer concentration function c is obtained.

$$c(t) = \frac{c_0}{AUC}\int_{-\infty}^{\infty} E(s, \bar{t}_1, Bo_1)_{ADM} E(t-s, \bar{t}_2, Bo_2)_{ADM} ds = c_0 E(t)_{TDM} \tag{18}$$

3. Results and discussion

3.1. Scale independent optimization strategy

A generalized approach for the optimization of a TSE process was developed based on the concept of Kolter et al. [29], which has been adjusted with respect to temperature management and process stability.

The main focus of this Scale Independent Optimization Strategy (SIOS) is the throughput expressed by the mass flow ṁ and the workload. These are linked by the specific feed load (Eq. (3)), which is a dimensionless surrogate for the fill level of the extruder and is defined as the ratio of mass flow to the generated volume by the rotation of the screws. This is given by the screw speed n and the external screw diameter D_a. The dimensionless form is derived by a transformation of the mass flow into a volume flow by the density ρ. This should ideally be the melt density. However, since this parameter is hard to determine the bulk density or crystal density is utilized, since this is relevant for the feeding mechanisms.

$$SFL = \frac{\dot{m}}{\rho n D_a^{\,3}} \tag{12}$$

The second considered variable is the melt temperature T_m at the extruder outlet, which is used as a measure for the applied thermal stress. This is linked to degradation, which is a crucial objective for product quality. T_m also reflects the material viscosity and is therefore connected to the flow conditions to a certain extend.

The overall process window for TSE optimization is stretched by these two parameters (see Fig. 2). However, material and machine limitations related to the desired application have to be respected as well. The exact position and course of the listed limitations is varying by the applied extruder, screw geometry and processed formulation and is given schematically.

In case of a solid dispersion production, the processing temperature has to be sufficient for plasticization of the material for the extrusion through the die. This is connected to the glass transition temperature T_g of the polymer, for partially crystalline material also the melting point has to be respected. The upper limit of the processing temperature is represented by the degradation temperature $T_{D,i}$ either of the API or the polymer. The lower one is crucial and typically related to the matrix carrier. This temperature range is also an indicator for the barrel temperature profile, which supports the unit operations in the individual zones, e.g. the melting of the material.

At low temperatures in the range of T_m the flowability of the formulation is poor. The available torque to force the material through the extruder is limited, which also restricts the load. The restriction of the process by the torque is at some point superseded by a maximum SFL. At the absolute limit the extruder would be completely filled. However, usually at some point the generated volume by the screws in combination with the transport effect is not sufficient enough anymore to process the mass flow. This limit is typically related to the intake zone, since the formulation is here in a powdery state and the density as well as flowability are the lowest.

The starting point (a) for the TSE optimization is chosen at a high screw speed and a low load with a melt temperature below the set limit. Step wise the load is maximized by keeping the screw speed constant and increasing the mass flow. Steady state operation should be reached at each level until the process parameters are changed again. The occurrence of a torque limit is an indicator to re-elect the starting point by increasing screw speed and mass flow pairwise. After reaching the maximum load (b) the SFL needs to be lowered by decreasing the mass flow for stable processing conditions (c). The degree of mass flow

reduction is dependent on the operator and the safety review. During this step the temperature profile is kept constant in order to support the process stability. A shut down of the barrel heating for autogenic (adiabatic) extrusion leads to a loss of process robustness, since the stability depends on constant processing conditions. However, in a production environment fluctuations of the periphery, e.g. of the feeders, are typical. Therefore, the heating is kept constant in order to support the endothermic mechanisms related to the material transformation during extrusion.

Finally, the throughput is maximized for a constant SFL by increasing mass flow and screw speed pairwise restricted by material properties (d) or e.g. the feeder (e). When the feeding is limited, the corresponding machine should be modified or replaced. For an overall limitation due to poor flowing conditions, e.g. at high drug loads, the formulation should be granulated beforehand to avoid a restriction of the process by this. Side feeding would be an additional option in this context.

3.2. Optimization results

The developed concept SIOS was applied for three different sizes of TSE extruders. According to the manufacturer, the melt temperature should not exceed 180 °C ($T_{max,set}$), while degradation indicated by a yellowing of the product respectively the polymer occurs above 200 °C ($T_{degradation}$). Therefore, the maximum temperature ($T_{barrel\ max}$) considered within the barrel temperature profile was chosen below these limits at 170 °C. The starting point (a) from the reference trials (ZSE 18) was transferred onto the other scales (ZSE 27 and ZSE 40) by keeping the screw speed and fill level constant and in consequence adapting the mass flow. The step width during the two parts of the SIOS procedure were based on the results for the reference extruder to the larger scales for reasons of comparability. The SIOS was applied (Fig. 3) three times at each scale with the same starting point. Steady state at each operating point was determined via process monitoring by the inline UV–VIS spectroscopy. In each process point the transmission signal also implied a successful production of an amorphous solid dispersion. The off-set of the spectra was not shifted as reported in [30], which is an direct indicator for crystal residues. Theoretically, this could be extended to an amorphous de-mixing, due to a change in the refractive index.

The application of the SIOS was successful for the ZSE 18. In the first part a limitation of the SFL was found according to material intake and a hold back in the hopper. This characteristic was also observed for the other machines after the same factorial increase of the starting point. The melt temperature for the maximization of the SFL was always in the range of the maximum barrel temperature at each step. This is an indicator for a dominant barrel heating in comparison to shear heating, which was enhanced for the experiments on the ZSE 27 and ZSE 40, indicated by the melt temperature exceeding the maximum set level. This deviation is related to two aspects. First of all, the surface to volume ratio is larger for smaller machine scales, which enables a higher efficiency for energy transfer at the inner barrel wall. On the other hand, the shear rate and the corresponding applied shear energy is higher for a larger screw diameter at a constant screw speed.

At all extruder sizes the maximizing of the throughput for a constant SFL led to an increasing melt temperature. This was related to a more dominant heating of the material by shear forces based on a higher screw speed, while the fill level remained identical in the extruder. For the reference extruder a final operating point (d) was defined, which fulfilled the prerequisites, while for the higher scales the manufacturer limit regarding the melt temperature was exceeded with the same number of optimization steps. The yellowing of the product occurred for the ZSE at (e), while these points symbolize an intake limit for ZSE 27 and ZSE 40. In both cases these operating points were unstable and

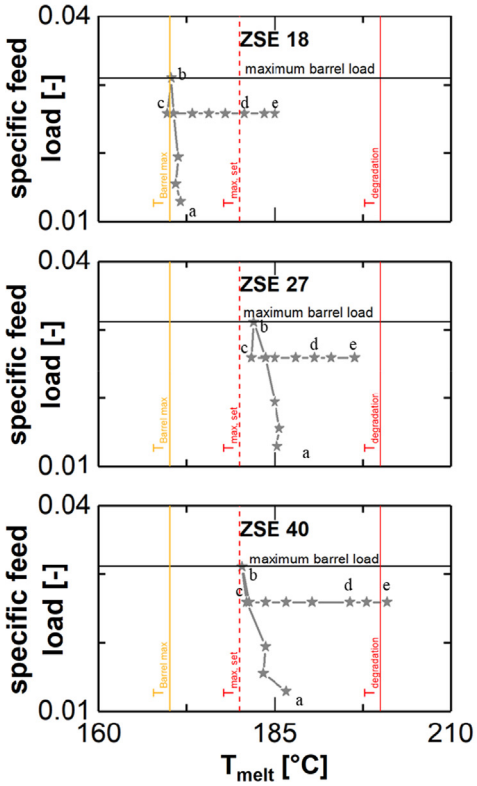

Pos	$\dot{m}$ [kg h^{-1}]	n [min^{-1}]	SFL [-]	T_{melt} [°C]
a	1.0	180	0.013	171.7±2.3
b	1.0	75	0.031	170.3±0.6
c	1.0	90	0.026	169.7±1.5
d	3.0	270	0.026	180.7±1.5
e	4.0	360	0.026	185.0±1.0
a	3.5	180	0.013	185.3±2.1
b	3.5	75	0.031	182.0±1.7
c	3.5	90	0.026	182.0±1.0
d	10.5	270	0.026	194.3±1.2
e	14.0	360	0.026	199.6±0.6
a	11.1	180	0.013	186.7±0.6
b	11.1	75	0.031	180.3±0.6
c	11.1	90	0.026	181.3±0.6
d	33.3	270	0.026	195.7±0.6
e	44.4	360	0.026	201.0±0.0

Fig. 3. Results of the SIOS applications displayed as process chart and corresponding process parameter for characteristic points. The procedure was executed in triplicate for each extruder. Variations of the melt temperature are displayed as mean average ± standard deviation.

material started to hold up in the hopper. Potentially the degassing area was not sufficient anymore, which led to a backwards flow of the water steam through the hopper.

3.3. RTD determination results

The impact on the RTD of maximizing the throughput at a constant SFL was documented for the application of the SIOS concept at the three extruder sizes. The RTD is expressed by the density function E and characterized by the quantiles t_i (Eq. (13)). These represent the time for the discharge of i wt% of the marker, which was added as a Dirac impulse.

$$\int_0^{t_i} E(t) = \frac{i}{100} \tag{13}$$

The experimental determination was executed for one run of the SIOS application at point (c) and three levels of it at a factorial increase of 2, 3 and 4 for the mass flow respectively screw speed at each extruder scale. The results and corresponding parameters are given in Fig. 4.

In each case, an enhanced mass flow corresponded to a faster transit of the material through the extruder, which is represented by shrinking quantile values as reaction to this variation. For t_{10} the extent of the reduction is equivalent to the reciprocal value of the factorial mass flow increase. This is in a good agreement with the modelling of TSE as a process driven by two mixing functions as in [31]. In [32] the first part of the RTD was identified as driven by a mechanism close to plug flow. Therefore, a mass flow increase results in reduction of the average transition time for a constant fill level by the same factor. This correlation is not valid for t_{50} and t_{90}, since the descending part of the RTD is driven by a mixing function related to the screw-barrel respectively screw-screw clearance [32].

Due to the Design of the SIOS application, the single set points of each stage correspond to a direct volumetric transfer between the different scales with respect to the ratio of the external screw diameters and a constant SFL. In comparison to the reference ZSE 18, the determined RTDs for the ZSE 27 are shifted to shorter transition times, while the time values for the ZSE 40 are slightly higher. This observations on the one hand is related to the ratio of external to inner screw diameter for each individual machine scale. This ratio ultimately defines the relative free inner volume within an extruder, which increases with a higher ratio. This parameter was not constant for the three utilized extruders (see Table 1). Therefore the real fill level was not identical, even though this is indicated by the SFL. This contrast is related to the definition of the SFL, which considers solely D_a as characteristic length and not the ratio D_a to D_i. Ultimately, with respect to the definition of the SFL the deviations correspond to a relative variation of ± 8%. Therefore the diameter ratio is not the single aspect for the deviations of the determined RTDs. A further influence parameter is potentially the excess pressure build-up due to the applied die plate and the real hold-up, which has to be differentiated from the fill level.

3.4. Comparison of the results for the different Scale-Up concepts

Within this study the smallest extruder scale ZSE 18 served as reference point for the application of the different Scale-Up approaches. The related mass flow and screw speed were determined beforehand by a scale independent optimization scheme for HME. For each Scale-Up concept the parameters are given for all in Table 2. In addition, the characteristic parameters barrel load/SFL and the total applied specific mechanical energy SME_{total} are listed. These are the main focus of the individual Scale-Up concepts.

The determined RTDs are presented for each approach by a representative run (Fig. 5), which is the closest to the average of three repetitions.

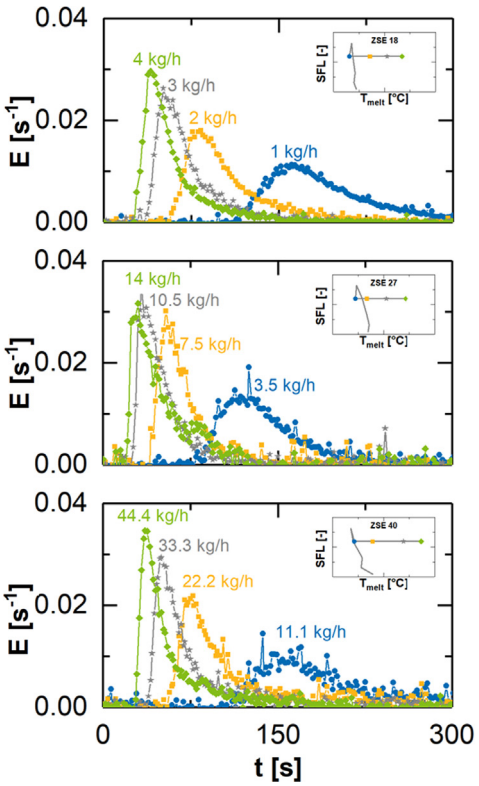

$\dot{m}$ [kg h^{-1}]	n [min^{-1}]	t_{10} [s]	t_{50} [s]	t_{90} [s]
1.0	90	140.3	179.9	261.1
2.0	180	71.2	95.6	161.5
3.0	270	45.4	62.8	110.3
4.0	360	34.7	49.6	98.1
3.5	90	100.1	131.8	200.2
7.0	180	48.1	64.5	119.8
10.5	270	30.4	44.2	82.5
14.0	360	24.9	40.1	77.0
11.1	90	135.1	180.9	311.2
22.2	180	68.4	89.8	175.2
33.3	270	45.6	61.8	135.3
44.4	360	33.0	47.0	110.9

Fig. 4. Determined RTD for a constant SFL and increasing mass flow at each applied extruder scale. Distributions are characterized by the specific quantile t_{10}, t_{50} and t_{90}.

Table 2
Overview about the Scale-Up experiments.

Extruder	Concept	ṁ [kg h^{-1}]	n [min^{-1}]	SFL [–]	SME_{total} [kWh kg^{-1}]
ZSE 18	Reference	3.0	270	0.026	0.402 ± 0.021
ZSE 27	SFL	10.5	270	0.026	0.432 ± 0.008
	aSFL	8.5	219	0.026	0.433 ± 0.008
	HT	6.9	270	0.017	0.595 ± 0.007
	SME	12.3	315	0.026	0.401 ± 0.008
ZSE 40	SFL	33.3	270	0.026	0.348 ± 0.006
	aSFL	22.3	181	0.026	0.376 ± 0.000
	HT	14.9	270	0.012	0.656 ± 0.023
	SME	27.5	270	0.020	0.403 ± 0.003

Table 3
Determined process parameters for the applied Scale-Up concepts.

Extruder	Concept	ṁ [kg h^{-1}]	T_{melt} [°C]	t_{50} [s]	Δp [bar]
ZSE 18	Reference	3.0	181 ± 2	63.4 ± 0.6	11 ± 0
ZSE 27	SFL	10.5	194 ± 1	46.5 ± 5.2	23 ± 1
	aSFL	8.5	192 ± 1	52.6 ± 1.0	23 ± 1
	HT	6.9	193 ± 1	67.2 ± 1.4	20 ± 1
	SME	12.3	196 ± 2	38.7 ± 0.4	23 ± 1
ZSE 40	SFL	33.3	197 ± 0	57.5 ± 0.4	14 ± 0
	aSFL	22.3	185 ± 1	86.6 ± 5.7	14 ± 0
	HT	14.9	194 ± 1	97.8 ± 8.9	10 ± 1
	SME	27.5	195 ± 2	70.6 ± 1.2	13 ± 0

On both extruder scales the geometric approaches can be categorized according to the considered power of D_a. The lowest residence times are connected to the SFL concept, while the highest values are obtained for the HT concept. In addition, a general shift to shorter residence times is found for the smaller scale. Consequently, the best agreement to the reference is visual for the HT concept on ZSE 27, while for the ZSE 40 this is achieved by the SFL concept. This inconsistency regarding the volumetric approaches is probably related to the different D_a/D_i-ratios. This defines the relative free volume inside an extruder and therefore the real free volume. For the ZSE 27 the D_a/D_i-ratio is smaller in comparison to the reference and this forces a general faster material transport. This is compensated by the Scale-Up concept with the smallest considered power of D_a, since this ultimately leads to a lower mass flow on the ZSE 27. However, subsequently the adjusted SFL is different for this approach in comparison to the reference process. On the ZSE 40 level the D_a/D_i-ratio is higher in comparison. Therefore the inner free volume is larger in relation, which leads to a relative deceleration of the material transport and the best agreement is found for the volumetric approach with the highest considered power of D_a and constant SFL in comparison the ZSE 18 process.

For the applied energetic Scale-up concepts no systematic results are obtained. While a constant SME_{total} results in a different RTD on the ZSE 27, the agreement to the reference is considered sufficient on the ZSE 40 level. In conclusion, neither a constant SFL nor a constant SME_{total} are in general crucial within this study for a sufficient Scale-Up regarding the preservation of the RTD.

3.5. Effect of Scale-Up concepts on the time location of the RTD

The mean residence time is considered crucial for pharmaceutical extrusion, since this parameter ultimately defines the general location in the time domain and the average duration of the multiple mechanisms during this process. A sufficient measure for this is the t_{50} quantile based on the density function E of the determined discrete RTDs (Table 3), which is the median of the distribution and typically considered for the average duration of an extrusion process.

With respect to the general variability of manually executed experiments for the determination of a RTD, a sufficient repeatability in each case is found for the three different runs at one parameter set-up. This is indicated by a relative standard deviation for the t_{50} values in the range of 1–6% (see Table 3). The higher deviations of 11% respectively 9% for the SFL-approach on the ZSE 27 level or the HT

Table 4
Determined model parameters for the data sets corresponding to the applied Scale-Up concepts.

Extruder	Concept	Bo_2 [–]	$\bar{t}_1$ [s]	$\bar{t}_2$ [s]	EBR [‰]
ZSE 18	Reference	1.39 ± 0.46	44.9 ± 2.2	11.9 ± 2.7	0.61 ± 0.04
ZSE 27	SFL	2.69 ± 1.47	28.0 ± 3.7	14.8 ± 3.0	1.24 ± 0.07
	aSFL	3.46 ± 0.41	31.1 ± 1.7	17.8 ± 1.5	1.22 ± 0.02
	HT	3.93 ± 0.41	31.6 ± 4.3	28.3 ± 6.4	0.81 ± 0.02
	SME	3.60 ± 0.08	22.4 ± 0.3	14.6 ± 0.3	1.38 ± 0.04
ZSE 40	SFL	1.10 ± 0.38	42.1 ± 2.2	9.2 ± 2.3	0.96 ± 0.02
	aSFL	1.10 ± 0.32	63.5 ± 5.2	13.1 ± 2.2	0.88 ± 0.00
	HT	3.77 ± 0.69	57.4 ± 1.1	35.5 ± 7.2	0.39 ± 0.03
	SME	0.86 ± 0.09	49.3 ± 0.9	11.1 ± 1.3	0.78 ± 0.01

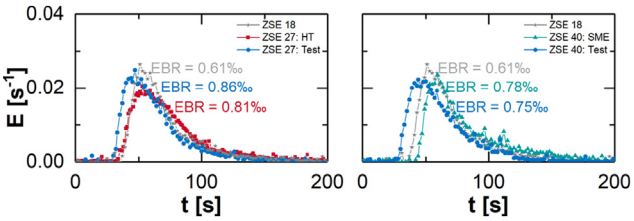

Fig. 6. Comparison of determined RTDs for test sets runs in retro perspective to the best fit of original Scale-Up experiments.

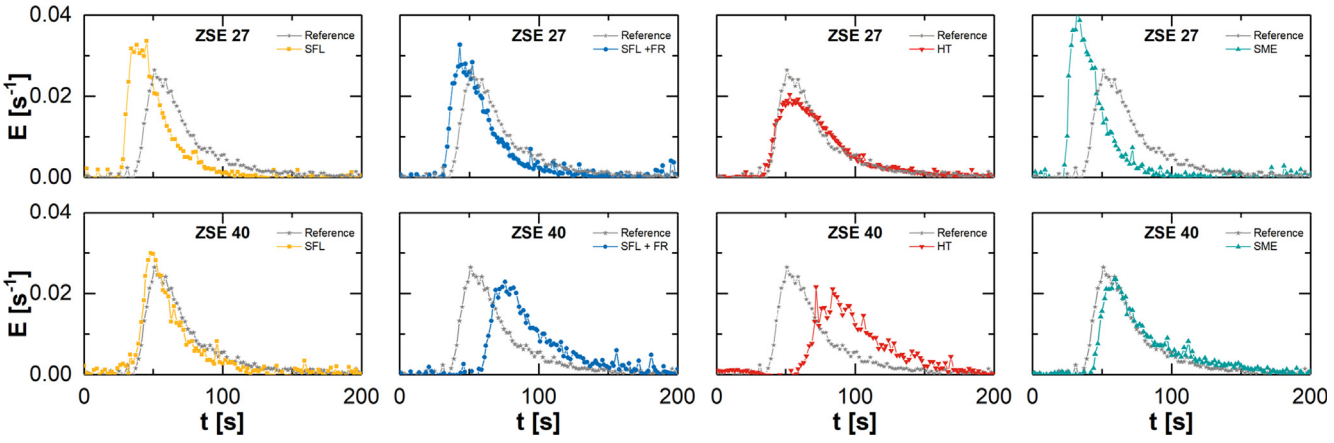

Fig. 5. Applied screw configuration and barrel temperature profile for the different extruder scales in.

approach on the ZSE 40 level are related to the disturbance of one run. However, still this variability is considered to be acceptable for experimental data sets.

The smallest deviations for the t_{50} of the reference to the RTDs for the applied Scale-Up concepts are connected on the ZSE 27 to the HT concept and on the ZSE 40 to the SFL and SME concept (see Table 3). This is in accordance to the visual impression.

At one extruder scale and for a constant SFL a higher mass flow leads to a shorter transport time, since the relative load of extruder remains unchanged and the transport velocity increases. In terms of process design, this is a potential operator action to adjust the minimum time for dissolving mechanisms, average time for reaction or to decrease the applied thermal and mechanical stress over time. A constant energy input has no systematic impact, since the mean residence time is shorter for the SME concept on the ZSE 27 scale, while the transport time is larger for the ZSE 40 scale.

The deviating load in case of the HT concept (see Table 2) for both extruder scales or for the SME concept applied on the ZSE 40 was compensated by a smaller pressure loss over the extrusion die. The pressure gradient influences the back pressure length [25] and thereby the hold-up in front of the die. However, this could not be avoided even by a scaling of the extrusion die with respect to the Hagen-Poiseullie law. The drawback in this case was the impact of the mass flow within this correlation, which varied for each scale-up concept, and the available equipment. Therefore a compromise for the incorporated extrusion die had to be made, which led to the different pressure gradients. In conclusion, the choice of the extrusion die affects the RTD for HME and consequently the processing conditions.

3.6. Evaluation of the RTD form

The TDM was fitted with Python 2.7.0 to the determined RTDs and the characteristic model parameters were obtained by the least square method. The results are presented in Table 4. The parameter Bo_1 is not listed, since all values exceed 100. Due to the enhanced sensitivity for this parameter towards deviations of data points from the theoretical course, the variation width for the fitted model parameter includes several decimal powers. However, this is negligible, since values over 100 are close to ideal plug flow.

For all Scale-Up concepts and the corresponding RTD data sets the parameter Bo_2 indicates an enhanced material backmixing with a duration time (t_2) shorter than the duration of the material transport. This leads to an asymmetric shape of the determined RTDs (see Fig. 5). A symmetric ratio of both mixing mechanisms is the highest for the HT concept on the ZSE 27, which is represented by the obtained model parameters and similar time parameters.

Overall, the best agreement to the reference is found for the SME-concept on the ZSE 40, while the agreement with the SFL and aSFL concept are also sufficient. Therefore the balance of the process mechanisms remains unchanged in comparison to the reference. The shift to higher time values for the aSFL approach is indicated by an increase of the model parameter $\tilde{t}_1$ and indicates an enhanced time e.g. for dissolving mechanisms, while the exposure time to thermal and mechanical stress is also enlarged. For the smaller extruder scale (ZSE 27) no fit considered sufficient is found according to the model parameters. However, the visual comparison (see Fig. 2) implies a sufficient agreement of the Scale-Up by the HT-approach to the reference.

A parameter, which also reflects transport and mixing during extrusion, is the EBR value. The deviation to the reference is the smallest for the HT approach on the ZSE 27 scale. The findings concerning the ranking of the Scale-Up concepts for the ZSE 40 level are also backed up by the EBR-values.

Therefore additional test sets were run in retro perspective to prove the relevance of the EBR value for the preservation of the RTD during scale-up. The results (Fig. 6) concerning the determined RTDs for these are illustrated in comparison to the reference (ZSE 18; grey) and the considered best fit on each scale. These are the HT-concept (red) on the ZSE 27 and the SME (turquoise) on the ZSE 40. The quality of the fits to the reference is considered equal.

4. Conclusion

Within this study a general strategy was presented for optimizing a Twin-Screw-Extrusion process with focus on maximizing the feed load and the throughput. This concept was applied for three different extruder scales. Therefore, the screw configuration as well as the barrel temperature profile was kept constant. The obtained results revealed similar operating windows with comparable limitations related to the maximum feed load, which was restricted by the intake mechanisms. While the temperature limitations were fulfilled for the reference extruder, the maximum melt temperature was exceeded for the larger scales for an identical procedure. This is related to a shift of the surface to volume ratio as well as impact of shear heating. The determined residence time distributions for a constant specific feed load indicated an enhanced plug flow for an increasing mass flow. Furthermore the results demonstrated the influence of the mass flow for a constant SFL.

The preservation during the Scale-Up from the reference extruder ZSE 18 to the higher level was successful for the Heat Transfer approach with respect to the energy balance ratio EBR and the location in the time domain represented by the t_{50} quantile. However, the fit of the corresponding data sets to the Twin-Dispersion-Model revealed a shift in the balance of material transport to shearing as an indicator for distributive mixing. For the ZSE 40 as next higher scale the approach concerning on a constant specific mechanical energy was most suitable. Moreover, the volumetric approaches with focus on a constant specific feed load and an advanced version with additional respect to a constant material intake mechanisms had also an overall sufficient agreement regarding the determined Residence Time Distribution to the reference extrusion process. These finding were both represented by the model fit and the EBR value.

Declaration of Competing Interest

The authors report no conflicts of interest. The authors alone are responsible for the content and writing of this article.

References

[1] M. Wilson, M.A. Williams, D.S. Jones, G.P. Andrews, Hot-melt extrusion technology and pharmaceutical application, Therapeut. Deliv. 3 (2012) 787–797.
[2] I. Major, C. McConville, Hot melt extruded and injection moulded dosage forms: Recent research and patents, Recent Pat. Drug Deliv. Formul. 9 (2015) 194–200.
[3] M. Tężyk, B. Milanowski, A. Ernst, J. Lulek, Recent progress in continuous and semi-continuous processing of solid oral dosage forms: A review, Drug Dev. Ind. Pharm. 42 (2015) 1195–1214.
[4] S.L. Lee, T.F. O'Connor, X. Yang, C.N. Cruz, S. Chatterjee, R.D. Madurawe, C.M.V. Moore, L.X. Yu, J. Woodcock, Modernizing pharmaceutical manufacturing: from batch to continuous production, J. Pharmaceut. Innovat. 10 (2015) 191–199.
[5] L.X. Yu, G. Amidon, M.A. Khan, S.W. Hoag, J. Polli, G.K. Raju, J. Woodcock, Understanding pharmaceutical quality by design, AAPS J. 16 (2014) 771–783.
[6] J.M. Juran, Juran on Quality by Design: The New Steps for Planning Quality into Goods and Services, Free Press, New York, NY, 1992.
[7] M. Li, C.G. Gogos, N. Ioannidis, Improving the API dissolution rate during pharmaceutical hot-melt extrusion I: Effect of the API particle size, and the co-rotating, twin-screw extruder screw configuration on the API dissolution rate, Int. J. Pharm. 478 (2015) 103–112.
[8] Y. Liu, M.R. Thompson, K.P. O'Donnell, Function of upstream and downstream conveying elements in wet granulation processes within a twin screw extruder, Powder Technol. 284 (2015) 551–559.
[9] G. Fukuda, B. Dryer, J. Webb, D.I. Bigio, M. Wetzel, P. Andersen (Eds.), Combinatorial effects of Kneading elements on mixing in twin-screw compounding, 2015.
[10] S.O. Carson, J.M. Maia, J.A. Covas, A new extensional mixing element for improved dispersive mixing in twin-screw extrusion, Part 2: experimental validation for immiscible polymer blends, Adv. Polym. Tech. 37 (2018) 167–175.
[11] M.A. Repka, S. Bandari, V.R. Kallakunta, A.Q. Vo, H. McFall, M.B. Pimparade, A.M. Bhagurkar, Melt extrusion with poorly soluble drugs - An integrated review, Int. J. Pharm. 535 (2018) 68–85.
[12] X. Zhang, H. Xing, Y. Zhao, Z. Ma, Pharmaceutical dispersion techniques for

dissolution and bioavailability enhancement of poorly water-soluble drugs, Pharmaceutics 10 (2018).
[13] Y.-Y. Chen, S.-Y. Zhang, Y.-H. Tao, Y. Wei, X.-D. Hu, Application of hot melt extrusion in the solid dispersion preparation of hydrophobic drugs: Research advances, J. Int. Pharmaceut. Res. 42 (2015) 593–600.
[14] J. Breitenbach, Melt extrusion: from process to drug delivery technology, Eur. J. Pharm. Biopharm. 54 (2002) 107–117.
[15] K. Nakamichi, T. Nakano, H. Yasuura, S. Izumi, Y. Kawashima, The role of the kneading paddle and the effects of screw revolution speed and water content on the preparation of solid dispersions using a twin-screw extruder, Int. J. Pharm. 241 (2002) 203–211.
[16] T. Villmow, B. Kretzschmar, P. Pötschke, Influence of screw configuration, residence time, and specific mechanical energy in twin-screw extrusion of polycaprolactone/multi-walled carbon nanotube composites, Compos. Sci. Technol. 70 (2010) 2045–2055.
[17] R.C. Evans, S.O. Kyeremateng, L. Asmus, M. Degenhardt, J. Rosenberg, K.G. Wagner, Development and performance of a highly sensitive model formulation based on torasemide to enhance hot-melt extrusion process understanding and process development, AAPS PharmSciTech 19 (2018) 1592–1605.
[18] A. Haser, S. Huang, T. Listro, D. White, F. Zhang, An approach for chemical stability during melt extrusion of a drug substance with a high melting point, Int. J. Pharm. 524 (2017) 55–64.
[19] A.L. Kelly, C. Kulkarni, T. Gough, R. Dhumal, A. Paradkar (Eds.), Melt extrusion of a pharmaceutical compound containing a poorly soluble thermolabile drug, 2012.
[20] D.E. Zecevic, R.C. Evans, K. Paulsen, K.G. Wagner, From benchtop to pilot scale–experimental study and computational assessment of a hot-melt extrusion scale-up of a solid dispersion of dipyridamole and copovidone, Int. J. Pharm. 537 (2018) 132–139.
[21] B. Chen, L. Zhu, F. Zhang, Y. Qiu, Process development and scale-up: Twin-screw extrusion, in: Developing Solid Oral Dosage Forms: Pharmaceutical Theory and Practice, second ed., 2016, pp. 821–868.
[22] B. Lang, J.W. McGinity, R.O. Williams III, Hot-melt extrusion-basic principles and pharmaceutical applications, Drug Dev. Ind. Pharm. 40 (2014) 1133–1155.
[23] J. Thiry, F. Krier, B. Evrard, A review of pharmaceutical extrusion: Critical process parameters and scaling-up, Int. J. Pharm. 479 (2015) 227–240.
[24] E. Reitz, H. Podhaisky, D. Ely, M. Thommes, Residence time modeling of hot melt extrusion processes, Eur. J. Pharm. Biopharm. 85 (2013) 1200–1205.
[25] K. Kohlgrüber, M. Bierdel (Eds.), Der gleichläufige Doppelschneckenextruder: Grundlagen, Technologie, Anwendungen, Hanser, München, 2007.
[26] B. Dryer, G. Fukuda, J. Webb, K. Montemayor, D.I. Bigio, P. Andersen, M. Wetzel, Comparison of scale-up methods for dispersive mixing in twin-screw extruders, Polym. Eng. Sci. 57 (2017) 345–354.
[27] J. Zierep, K. Bühler (Eds.), Grundzüge der Strömungslehre: Grundlagen, Statik und Dynamik der Fluide : mit zahlreichen Übungen, 10th ed., Springer Vieweg, Wiesbaden, 2015.
[28] I. Ghosh, R. Vippagunta, S. Li, S. Vippagunta, Key considerations for optimization of formulation and melt-extrusion process parameters for developing thermosensitive compound, Pharm. Dev. Technol. 17 (2012) 502–510.
[29] K. Kolter, M. Karl, A. Gryczke, Hot-melt Extrusion with BASF Pharma Polymers: Extrusion Compendium, second ed., BASF, Ludwigshafen, 2012.
[30] J. Wesholowski, S. Prill, A. Berghaus, M. Thommes, Inline UV/Vis spectroscopy as PAT tool for hot-melt extrusion, Drug Deliv. Translat. Res. 8 (2018) 1595–1603.
[31] J. Wesholowski, H. Podhaisky, M. Thommes, Comparison of residence time models for pharmaceutical twin-screw-extrusion processes, Powder Technol. (2018).
[32] J. Wesholowski, A. Berghaus, M. Thommes, Investigations concerning the residence time distribution of twin-screw-extrusion processes as indicator for inherent mixing, Pharmaceutics 10 (2018).
[33] G.I. Taylor, Diffusion and mass transport in tubes, Proc. Phys. Soc.. Section B 67 (1954) 857–869.
[34] K.B. Bischoff, O. Levenspiel, Fluid dispersion—generalization and comparison of mathematical models—II comparison of models, Chem. Eng. Sci. 17 (1962) 257–264.